BIOCHEMISTRY
including biophysical chemistry & molecular biology

ARTICLE

pubs.acs.org/biochemistry

Quantification of Cysteinyl S-Nitrosylation by Fluorescence in Unbiased Proteomic Studies

John E. Wiktorowicz,[*,†,‡,§] Susan Stafford,[‡] Harriet Rea,[†] Petri Urvil,[∥] Kizhake Soman,[†,‡,§] Alexander Kurosky,[†,‡,§] J. Regino Perez-Polo,[†,§] and Tor C. Savidge[∥]

[†]Department of Biochemistry and Molecular Biology, [‡]National Heart, Lung, and Blood Institute Proteomics Center, [§]Sealy Center for Molecular Medicine, and [∥]Department of Internal Medicine-Gastroenterology, The University of Texas Medical Branch, Galveston, Texas 77555, United States

Supporting Information

ABSTRACT: Cysteinyl S-nitrosylation has emerged as an important post-translational modification affecting protein function in health and disease. Great emphasis has been placed on global, unbiased quantification of S-nitrosylated proteins because of physiologic and oxidative stimuli. However, current strategies have been hampered by sample loss and altered protein electrophoretic mobility. Here, we describe a novel quantitative approach that uses accurate, sensitive fluorescence modification of cysteine S-nitrosylation that leaves electrophoretic mobility unaffected (SNOFlo) and introduce unique concepts for measuring changes in S-nitrosylation status relative to protein abundance. Its efficacy in defining the functional S-nitrosoproteome is demonstrated in two diverse biological applications: an in vivo rat hypoxia-ischemia/reperfusion model and antimicrobial *S*-nitrosoglutathione-driven transnitrosylation of an enteric microbial pathogen. The suitability of this approach for investigating endogenous S-nitrosylation is further demonstrated using Ingenuity Pathways analysis that identified nervous system and cellular development networks as the top two networks. Functional analysis of differentially S-nitrosylated proteins indicated their involvement in apoptosis, branching morphogenesis of axons, cortical neurons, and sympathetic neurites, neurogenesis, and calcium signaling. Major abundance changes were also observed for fibrillar proteins known to be stress-responsive in neurons and glia. Thus, both examples demonstrate the technique's power in confirming the widespread involvement of S-nitrosylation in hypoxia-ischemia/reperfusion injury and in antimicrobial host responses.

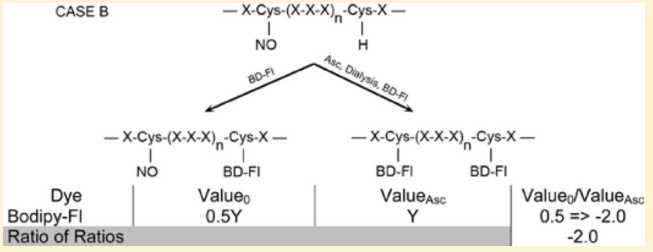

The discovery of nitric oxide (NO) as a regulator of cellular redox is of universal importance, particularly because of its impact on signal transduction.[1−4] Cysteinyl S-nitrosylation (SNO) is a major mechanism by which NO modulates protein activity, and it is now increasingly appreciated that aberrant S-nitrosylation of specific molecular targets contributes to disease pathogenesis. Consequently, there is much interest in developing methods that quantify altered protein S-nitrosylation for investigative studies and clinical diagnosis.

Several approaches have been developed to gauge the degree of SNO modifications, including chemiluminescence[5] and colorimetric[6] methods; however, detection of SNO and identification of modified proteins were truly enabled by the development of the "biotin-switch technique" (BST).[7,8] This extensively utilized method represents the gold standard for the identification of protein SNO and uses biotin as an affinity ligand or biotin linked to a fluorescent probe to additionally confer quantification, together with a thiol-reactive functional group for the purification of sulfhydryl-containing proteins. Since the development of the BST, several modifications have been developed to gauge the degree and impact of SNO on biochemical processes, including the incorporation of stable isotope or fluorescent labels.[1,3,9] However, all of these approaches use methyl methanethiosulfonate (MMTS) to first S-alkylate free protein thiols. This is followed by removal of NO from cysteine by ascorbate (Asc) treatment. The resultant cysteine is then alkylated by the S-reactive agent attached to biotin and can then be purified by affinity adsorption with streptavidin.

Several difficulties have arisen, however, that impact the efficacy and accuracy of the BST approach when applied to unbiased proteomic analysis. Some of the more important issues include alteration of the electrophoretic mobility of proteins by biotin, rendering global differential analysis difficult. The increase or decrease in signal intensity may also be due to altered protein abundance, not only a change in SNO levels. For fluorescently labeled BST, quantitative accuracy is impacted by protein losses that occur from multiple precipitations and streptavidin elution. Additional problems relate to the use of MMTS and Asc, as well

Received: January 4, 2011
Revised: May 25, 2011
Published: May 26, 2011

as recent modifications to the original method, including alternative labeling strategies.[1,6,10] In many respects, the efforts to globally quantify and identify proteins that undergo SNO mirror those in pursuit of the same goals in discovery proteomics. Chemical modification with a reporter group that permits quantification (and/or normalization for losses), separation, isolation, and identification of significantly abundant proteins underlies most of these efforts.

We have recently developed a strategy that accomplishes these goals with minimal impact on the chemical behavior of proteins using saturation fluorescence labeling of cysteines for accurate quantification of proteins separated by two-dimensional gel electrophoresis (2DE) in discovery proteomics investigations.[11,12] Further, we have modified this approach to study the global impact of respiratory syncytial virus (RSV) infection on reactive oxygen formation and the protective effects of human lung epithelial cell-derived peroxiredoxin (Prdx) 1 and 4. In that proteomic study, we identified 15 uniquely oxidized proteins following RSV infection and Prdx knockdown.[13]

Here, we report a novel strategy for specifically labeling, detecting, and quantifying protein SNO by fluorescence saturation (SNOFlo). In this approach, the total cysteine content of the cell extracts is determined by amino acid analysis, followed by denaturation and division of the extract into two equal fractions. One fraction is labeled with a 60-fold excess of BODIPY FL-maleimide (BD), an uncharged cysteine-specific fluorescent dye, under conditions that minimize nonspecific modifications,[11] and the second fraction is treated with Asc to reverse the SNO modification and is likewise labeled with BD. Subsequent 2DE with fluorescence quantification permits the ratiometric determination of protein regulation between control and experimental samples treated with Asc, as well as the ratiometric determination of the change in SNO in the fractions not treated with Asc. This "ratio of ratios" yields the change in SNO normalized to the change (if any) in protein abundance. For example, after experimental stimulus, proteins not treated with Asc that demonstrate lower fluorescence compared to controls are indicative of increased SNO (i.e., labeling blocked by SNO) induced by the experimental stimulus. Examination of the same proteins after Asc-mediated reversal reveals the up- or downregulation of the protein itself (when compared to controls). Thus, the ratio of Asc-treated to untreated controls and experimentals reveals whether an increased (or decreased) signal intensity is the result of altered protein abundance or S-nitrosylation status. The ability to perform these analyses, therefore, is uniquely dependent on the uncharged nature of the dyes and their lack of influence on the modified protein pI values, permitting spot matching in 2DE between Asc-treated and untreated samples, and saturation fluorescence labeling, permitting accurate and sensitive quantification of SNO-modified proteins, regardless of their SNO modification or labeled state.

We present here two biological examples of the use of SNOFlo to estimate and identify the degree of SNO in proteins discovered in an unbiased evaluation of cell-driven nitrosylation in a hypoxia-ischemia (HI) /reperfusion (HHI) rat model, and externally S-nitrosylated proteins [via S-nitrosylated glutathione (GSNO)].

EXPERIMENTAL PROCEDURES

Neonatal Hypoxia-Ischemia and Hyperoxia Treatment. Pregnant Wistar rat dams (Charles River Laboratories, Wilmington, MA) were allowed to deliver spontaneously. On day P1, the litters were culled to 10 pups and randomly mixed among two dams (having a total of 20 pups per experiment). On day P7, all pups were removed from the dam, weighed, sexed, and randomly assigned to one of four groups: sham, HI, HI with extreme hyperoxia treatment (100% oxygen, HHI 100%), or HI with moderate hyperoxia treatment (40% oxygen, HHI 40%). HI was induced as previously described by Rice et al.[14] and modified by Grafe et al.[15] Briefly, in a 37 °C E-Z anesthesia chamber (Euthanex Corp., Palmer, PA), day P7 rat pups were anesthetized with isofluorane (5% for induction and 2% for maintenance) balanced with 100% O_2 blood-gas grade. The left carotid artery was isolated after a midneckline incision and permanently ligated by electrocauterization. After being anesthetized, the sham surgical pups received a midneckline incision and were immediately sutured and cleaned. The sham pups were not subjected to common carotid artery isolation to prevent minor ischemia/reperfusion events. All pups were then returned to their dams for a recovery period of 90 min. After recovery, the sham pups were placed in a normoxia chamber at 37 °C and the ischemic pups were placed in a 37 °C humidified hypoxia chamber (8% oxygen balanced with blood-gas grade nitrogen) where systemic hypoxia was induced for 90 min.[16−19] A cohort of these pups also received extreme (100% blood-gas grade O_2) or moderate (40% O_2 balance with blood-gas grade nitrogen) hyperoxia treatment at 37 °C immediately after HI for a period of 120 min. Sham and HI-treated pups were kept at 37 °C normoxia for the length of time of the hyperoxia treatment. Immediately after, the pups were returned to their dams until their assigned survival time point.

Preparation of Rat Brain Extracts. Pups were deeply anesthetized with isofluorane and then decapitated. The whole brains were removed, and ipsilateral cortices (from the anterior tuber cinereum to the anterior of the occipital cortex, encompassing the parietal cortex) were collected one day after the insult.

Preparation of Bacterial Protein Extracts. Enteropathogenic *Escherichia coli* (EPEC) E2348/69 cells[20] were grown in 100 mL of LB medium at 37 °C with shaking for 3 h until late log phase (OD_{600} = 0.8−1.0). The cells were centrifuged at 4 °C for 30 min at 3200*g* and washed once with 15 mL of cold PBS containing 1 mM EDTA and 0.1 mM diethylenetriaminepentaacetic acid (DTPA) (Sigma, St. Louis, MO). The supernatant was removed, and the protein fraction was prepared with chloroform-hypotonic shock as described previously.[21] Briefly, the cell pellet was resuspended in the residual medium; 30 μL of chloroform was added, and the cells were vortexed and kept at room temperature (RT) for 5 min. Then 10 mL of cold 10 mM Tris (pH 7.4) containing a cocktail of protease inhibitors (Complete EDTA-free, Roche, Indianapolis, IN) was added, and the mixture was vortexed. The resulting extract was centrifuged at 22000*g* for 10 min at 4 °C. The extracted proteins in the supernatant were precipitated at −20 °C for 1 h with 4 volumes of cold 100% acetone and pelleted for 30 min at 4 °C and 3200*g*.

Probing Bacterial Proteins with Cysteines Available for SNO. All procedures, including GSNO treatment, S-alkylation, and reduction, were performed away from direct sunlight. The details have been published previously[22] and are presented here briefly. Before GSNO treatment of proteins under native non-reducing conditions (1−100 μM), proteins were resuspended at a concentration of 2 mg/mL with 50 mM HEPES (pH 7.7) containing 1% zwitterionic detergent CelLytic B (Sigma), 1 mM

EDTA, 0.1 mM neocuproine (Sigma), and protease inhibitors (Roche). Protein extracts were treated with 1, 10, or 100 μM GSNO at RT for 40 min with mild shaking. The untreated control and the GSNO-treated protein fractions were precipitated with 100% acetone as described above and washed three times with cold 70% acetone.

To block the free thiols, the pellets were resuspended at 0.8 mg of protein/mL in 200 mM HEPES (pH 7.7) containing 20 mM *S*-methylmethane thiosulfonate (MMTS), 1 mM EDTA, 0.1 mM neocuproine, and 2.5% SDS. The suspensions were incubated at 50 °C for 40 min with vortexing at 10 min intervals. Excess MMTS was then removed by precipitating the proteins with 100% acetone and washing three times with cold 70% acetone as described above.

To reduce the SNO's to thiols, the washed protein pellets were resuspended in 0.5 mL of 50 mM HEPES buffer containing 1% SDS and 1 μM CuCl, and 0.5 mL of SNO Reducing Reagent (S-Nitrosylated Protein Detection Kit, Cayman Chemical Co., Ann Arbor, MI), and the reducing reactions were conducted at RT with mild shaking for 1 h. Subsequently, the proteins were precipitated with 100% acetone as described above. As a specificity control, SNO photolysis was used to demonstrate protein SNO as described previously.[41]

Lowering the SDS Concentration for 2DE. To lower the SDS concentration of the protein samples, the pellets were resuspended in 0.5 mL of 50 mM HEPES (pH 7.7), 1 mM EDTA, 0.1 mM neocuproine, and 0.1% SDS. Then 3 volumes (1.5 mL) of neutralization buffer (NB) [50 mM HEPES (pH 7.7), 100 mM NaCl, 1 mM EDTA, and 1% Triton X100] was added. The proteins were precipitated by adding 4 volumes of cold 100% acetone, and the suspension was incubated at RT for 20 min before being centrifuged at 22000*g* and 7 °C for 5 min. The pellet was resuspended in 1.2 mL of NB (an aliquot was taken for the BCA protein assay), and the suspension was precipitated with 100% acetone as described above. The pellet was washed twice with 70% RT acetone. The samples were then processed for BD labeling and 2DE.

Biotin-Switch Technique with Streptavidin Pull-Down. In part of the samples, the SNO groups of the proteins were switched to biotin by including SNO Labeling Reagent (Cayman Chemical Co.) in the SNO Reducing Reagent. The reducing and labeling reactions were conducted at RT with mild shaking for 1 h. Subsequently, the proteins were precipitated with 100% acetone. The pellets were resuspended in 0.5 mL of 50 mM HEPES (pH 7.7), 1 mM EDTA, 0.1 mM neocuproine, and 0.1% SDS. To perform the streptavidin pull-down, 250 μL of the suspension was diluted with 750 μL of NB. This solution was tumbled oovernight at 4 °C with 30 μL of streptavidin agarose beads, which had been prewashed with NB. The beads were pelleted at 200*g* for 30 s, washed with NB containing 600 mM NaCl, and pelleted. The pellet was then treated for two-dimensional (2D) analysis.

Cysteine Saturation Fluorescence Assay (SNOFlo) for 2D Gel Separations and Analyses of the S-Nitrosoproteome. Amino acid analysis (Hitachi) was used to determine the total cysteine content of the protein sample. Protein (400 μg) in 7 M urea, 2 M thiourea, 2% CHAPS, and 50 mM Tris (pH 7.5) was labeled with BODIPY FL *N*-(2-aminoethyl)maleimide (Life Technologies, Inc., Carlsbad, CA) at a 60-fold excess of cysteine to BODIPY FL-maleimide (BD) as described previously.[11] Protein samples from the rat HHI model were treated with Asc to reverse SNO and then dialyzed against the urea buffer to remove Asc, which interferes with labeling. Bacterial samples were labeled directly after dissolution in the urea buffer. After the labeling reaction had been quenched with a 10-fold molar excess of β-mercaptoethanol (BD:βME), 200 μg of labeled protein in 0.5% IPG buffer (pH 3−10) (GE Healthcare) was loaded onto a 11 cm pH 3−10 IPG strip (GE Healthcare) in duplicate, and proteins were focused according to the following protocol: (1) 50 V for 11 h (hydration of strip), (2) 250 V for 1 h, (3) 500 V for 1 h, (4) 1000 V for 1 h, (5) 8000 V for 2 h (steps 2−5 are gradient increases in voltage), and (6) 8000 V × 48000 V/h. After focusing, the IPG strips were equilibrated in 6 M urea, 2% SDS, 50 mM Tris (pH 8.8), and 20% glycerol for 30 min at RT, applied to an 8 to 16% Tris-glycine-SDS gel, and run at 150 V for 2.25 h at 4 °C. The gels were fixed for 1 h in 10% methanol and 7% acetic acid and washed overnight in 10% ethanol. Finally, gels were imaged on a ProXpress 2D Proteomic Imaging System [Perkin-Elmer; excitation λ = 480 nm (40 nm bandpass), and emission λ = 535 nm (50 nm bandpass)]. We have previously demonstrated that this covalent sulfhydryl alkylation method using an uncharged thiol-reactive dye exhibits excellent specificity for cysteine thiols (with little to no modification of other amino acid residues), does not impact protein electrophoretic mobility (for spot matching with unlabeled proteins), and accomplishes highly accurate and reproducible quantification (by virtue of its specificity and saturating concentration over protein thiols).[11,23] Finally, the label does not interfere with high-confidence mass spectrometric identification of proteins, while exploiting the linearity of detection and labeling[11] and inherent sensitivity of fluorescence detection. With respect to the latter, we have established the limit of detection of our fluorescence imager (PE ProExpress 2D) of singly labeled enolase (one cysteine) to be 0.6 fmol/protein spot (unpublished observations), a sensitivity equivalent to roughly 1500 copies of a given protein from 200000 cells (our typical protein load for a discovery 2DE experiment).

Protein Quantification and Image Analysis. The 2DE images were analyzed using Progenesis/SameSpots (Nonlinear Dynamics, Ltd., Newcastle Upon Tyne, U.K.). The current version of Progenesis SameSpots, unlike traditional analysis, does not rely on propagating and matching spots to an arbitrary reference. Instead, it relies on geometric correction of the scans themselves and projecting them all into the same reference space, performing pixel-to-pixel matching before spot detection. This approach ensures that spot boundaries are the same for all gels, eliminating errors that accumulate in the reference gel(s) as the number of gels within one experiment increases. Once the pixel matching and spot detection are complete, a reference gel is selected according to several criteria, including the quality and number of spots. Subsequent to automatic spot detection, spot filtering is manually performed and spots with an area of less than 250 pixels are filtered out, and spots with a volume (intensity): area ratio of less than 375 pixels (whose abundance is insufficient for MS identification) are also filtered. Typically, some manual spot editing is required to correct for spots that are not split correctly, not detected, or split unnecessarily during the automated detection process. The matching of spots between the gels is manually reviewed and adjusted as necessary. The software normalizes spot volumes using a calculated bias value based on the assumption that the great majority of spot volumes represent no change in abundance (ratio of control to experimental = 1.0) (Nonlinear Dynamics documentation).

Calculation of the Ratio of Ratios and Oxidation Protection Index. Because the purpose of this study is to establish a method for identifying proteins whose cysteines have undergone modification due to an experimental treatment, it is critical to differentiate the cellular response of changing protein expression versus changing S-modification. However, because both are measured by the fluorescence intensity of the cysteine-bound fluorophore, it was necessary to measure the fluorescence intensity before and after treatment with Asc. Hence, the abundance ratios of proteins with and without Asc treatment and within each experimental and control sample were calculated. From these, a ratio of ratios was calculated as follows:

$$\text{ratio of ratios} = \frac{\Delta[\text{Cys-NO}]}{\Delta[\text{protein}]} = \frac{[\text{BD}^{\text{Exp}}_{\text{Asc}-}/\text{BD}^{\text{Ctrl}}_{\text{Asc}-}]}{[\text{BD}^{\text{Exp}}_{\text{Asc}+}/\text{BD}^{\text{Ctrl}}_{\text{Asc}+}]}$$

where BD is the normalized BODIPY fluorescence intensity of a protein spot, Asc^- denotes a lack of Asc treatment, Asc^+ denotes Asc treatment, Exp denotes HI or HHI, and Ctrl denotes control.

Thus, the ratio of ratios reflects the degree of cysteinyl oxidation relative to the total protein abundance for that protein spot. The change in the ratio of ratios across the experiment is defined as the oxidation protection index (PI). A negative value is indicative of an increase in the level of oxidation (lower normalized BD fluorescence), while a positive value represents a decreased level of oxidation (higher normalized BD fluorescence).

Statistical Analysis and Database Interrogation.. Normalized spot volume ratios across samples were calculated, and ANOVA and *q*-value analyses [permitting false discovery (FDR) for the selected population of proteins to be calculated][24] generated by SameSpots were used to select protein spots for MS identification and correlation analyses. Normalized spot volumes greater than ±1.3-fold ($p < 0.05$) were considered significantly changed, and these spots were subsequently robotically picked and digested with trypsin.

Hierarchical clustering was performed using unweighted average (UPGMA) as the clustering method, Euclidean distance as the similarity measure, and average value as the ordering function. A heat map was generated using Spotfire 9.1 (TIBCO Software Inc., Palo Alto, CA). The standardized spot volumes (V) from SameSpots for the significant spots were first normalized by being converted to Z scores. This involved calculation of the Z score for each spot, i, in every sample, as $Z_i = (V^i - \mu)/\sigma$, where μ and σ are the mean and standard deviation, respectively, across all samples for that spot. The average Z score for a spot across all of the samples is equal to zero; therefore, positive and negative values denote above and below average protein abundance, respectively. The Z scores are depicted graphically in the form of a heat map with the rows representing the different proteins (spots) and columns the different samples.

Protein Identification and Database Interrogation. Protein gel spots were excised and prepared for MALDI TOF/TOF analysis using Genomic Solutions' ProPic II and ProPrep robotic instruments (DigiLab, Ann Arbor, MI) following the manufacturer's protocols. Briefly, gel pieces were incubated with trypsin [20 μg/mL in 25 mM ammonium bicarbonate (pH 8.0) (Promega Corp.)] at 37 °C for 4 h.

Matrix-assisted laser desorption ionization time-of-flight mass spectrometry (MALDI TOF-MS) was used to analyze the samples and identify proteins. Data were acquired with an Applied Biosystems 4800 MALDI TOF/TOF Proteomics Analyzer. The Applied Biosystems software package included a 4000 Series Explorer (v. 3.6 RC1) with Oracle Database Schema (version 3.19.0) and Data (version 3.80.0) to acquire both MS and MS/MS spectral data. The instrument was operated in positive ion reflectron mode; the mass range was 850−3000 Da, and the focus mass was set at 1700 Da. For MS data, 2000−4000 laser shots were acquired and averaged from each sample spot. Automatic external calibration was performed using a peptide mixture with reference masses of 904.468, 1296.685, 1570.677, and 2465.199.

Following MALDI MS analysis, MALDI MS/MS was performed on several (5−10) abundant ions from each sample spot. A 1 kV positive ion MS/MS method was used to acquire data under post-source decay (PSD) conditions. The instrument precursor selection window was ±3 Da. For MS/MS data, 2000 laser shots were acquired and averaged from each sample spot. Automatic external calibration was performed using reference fragment masses of 175.120, 480.257, 684.347, 1056.475, and 1441.635 (from a precursor mass of 1570.700).

Applied Biosystems GPS Explorer (version 3.6) was used in conjunction with MASCOT to search the respective protein database using both MS and MS/MS spectral data for protein identification. Protein match probabilities were determined using expectation values and/or MASCOT protein scores. MS peak filtering included the following parameters: mass range of 800−4000 Da, minimum signal-to-noise (S/N) filter of 10, mass exclusion list tolerance of 0.5 Da, and mass exclusion list (for some trypsin and keratin-containing compounds) that included masses of 842.51, 870.45, 1045.56, 1179.60, 1277.71, 1475.79, and 2211.1. For MS/MS peak filtering, the minimum S/N filter equaled 10.

For protein identification, the relevant taxonomy was searched in the NCBI database. Other parameters included the following: selecting the enzyme as trypsin; maximum number of missed cleavages, 1; fixed modifications included BD (C) for 2D gel analyses only; variable modifications included oxidation (M); precursor tolerance set to 0.2 Da; MS/MS fragment tolerance set to 0.3 Da; mass, monoisotopic; and peptide charges only considered as +1. The significance of a protein match, based on both the peptide mass fingerprint (PMF) in the first MS and the MS/MS data from several precursor ions, is based on expectation values; each protein match is accompanied by an expectation value. The expectation value is the number of matches with equal or better scores that are expected to occur by chance alone. The default significance threshold is $p < 0.05$, so an expectation value of 0.05 is considered to be on this threshold. We used a more stringent threshold of 10^{-3} for protein identification; the lower the expectation value, the more significant the score.

RESULTS

General Strategy and Approach. Current approaches to estimating SNO in an unbiased proteomics experiment may yield misleading results because cells may respond to challenge by modulating protein synthesis, as well as altering their proteins via post-translational modifications. S-Nitrosylation of cysteines lends itself to gauging the separate contributions of each cellular response by virtue of its reversibility; i.e., differential analyses against controls can be performed before Asc-mediated SNO reversal to measure SNO, and after reversal to estimate overall experimentally induced changes in protein abundance (in this case hypoxia/reperfusion). Expressing the protein abundances as

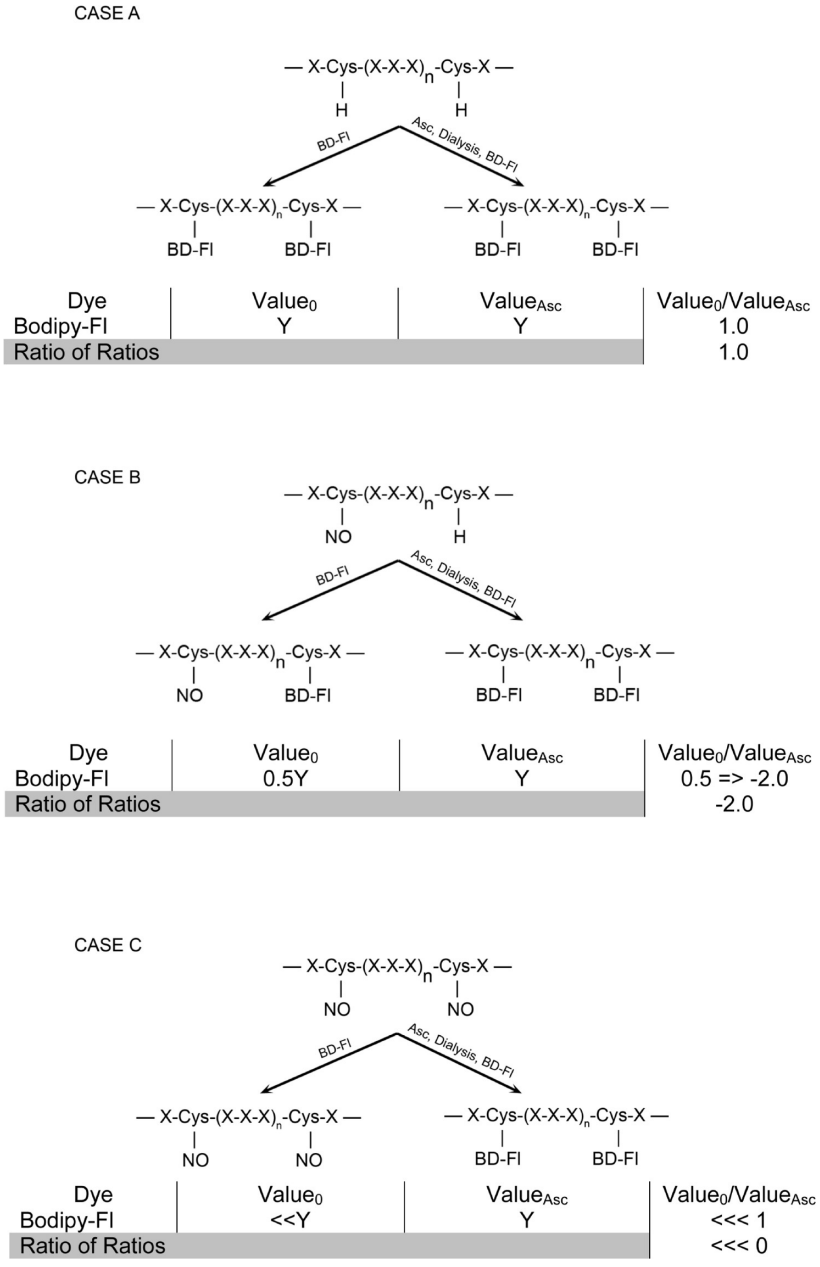

Figure 1. Schematic of saturation fluorescence labeling with cysteine-specific BODIPY FL-maleimide (BD) dye. Three cases are presented focusing on the degree of cysteine modification that can be reversed by Asc (i.e., S-nitrosylation). All assume that the protein abundance does not change with the treatment. Case A demonstrates a canonical protein structure with no cysteine S-nitrosylation before treatment with BD, after labeling, and after Asc treatment and labeling. No change in protein spot fluorescence will be observed unless the protein abundance changes. This is quantified by the ratios of ratios as described in Experimental Procedures. Case B demonstrates the partial S-nitrosylation after treatment and the resultant ratio of ratios upon Asc treatment and labeling. Here ratios of <1 are expressed as the negative reciprocal. Case C demonstrates the complete S-nitrosylation and the ratio of ratios after Asc reversal. If the protein abundance changes due to the HI or HHI treatment, with or without S-nitrosylation, the ratio of ratios will normalize the values.

a ratio of intensities yields an estimate of SNO relative to the specific protein abundance across the experiment (Figure 1). Accomplishing this, however, requires that the protein mobility not be dependent upon the state of cysteine modification (SNO or fluorescence-labeled); otherwise, matching and quantification of proteins across the experiment will be problematic.

In Figure 1, we examine three hypothetical circumstances (cases A−C), each reflecting differing degrees of SNO. Each case assumes no change in protein abundance across the experiment; however, the ratio of ratios eventually normalizes any changes. Case A describes a protein with no SNO, where all cysteines are modified, resulting in a strong fluorescence signal. The ratio of intensities before and after Asc treatment remains at 1.0 because the protein abundance does not change.

Case B illustrates partial cysteinyl S-nitrosylation where the fluorescence intensity reflects the unmodified fraction before Asc treatment. After Asc treatment, all cysteines are labeled; hence, the ratio reflects the fraction of SNO. Because the ratio of ratios is

dx.doi.org/10.1021/bi200008b |*Biochemistry* 2011, 50, 5601–5614

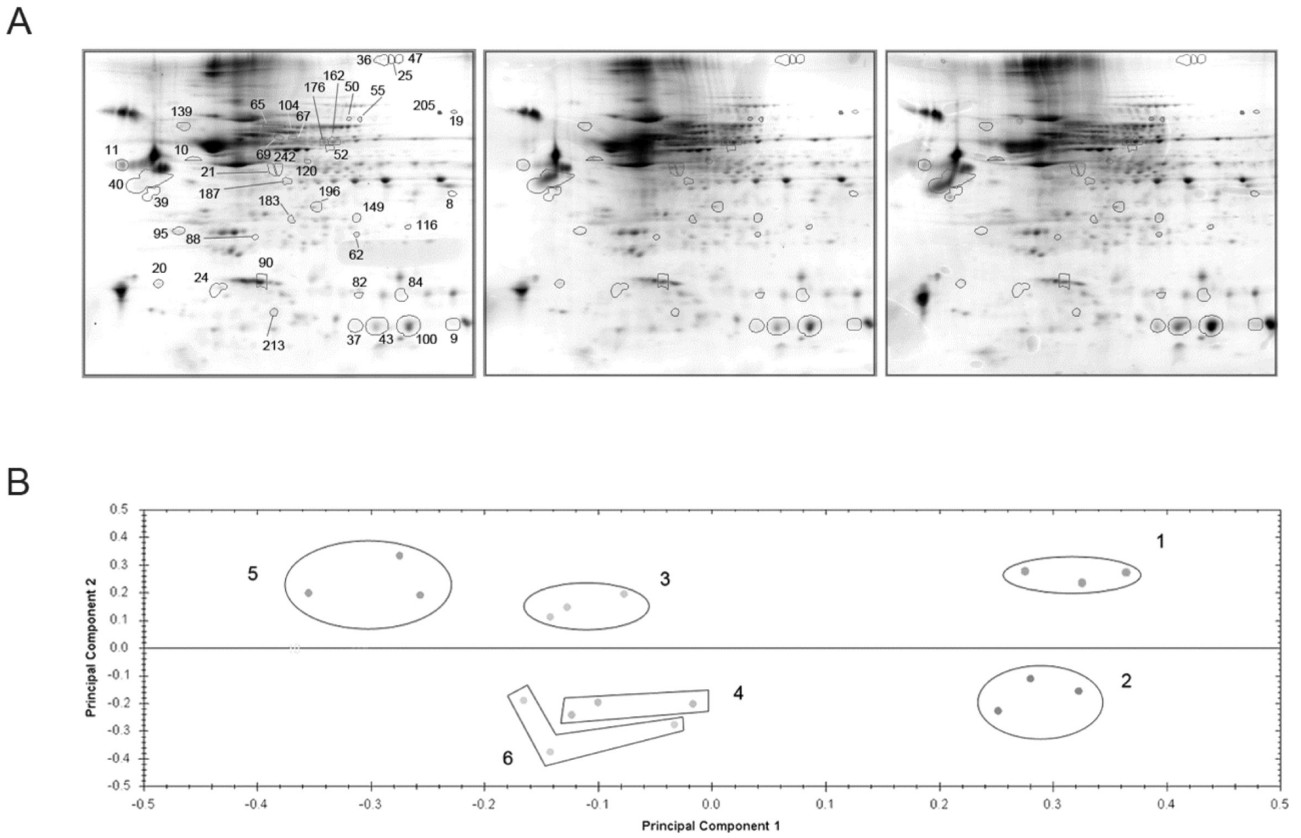

Figure 2. (A) HHI two-dimensional gel separations. Representative gels from (left to right) the control, HI, and HHI triplicate samples are shown with the 41 proteins demonstrating significant ratio of ratio responses. Details are described in the text. (B) Principal component analysis (PCA) of the protein spot intensities. PCA of the 41 protein spots (IDs are presented in Table 1). Principal component 1 represents controls vs HI and HHI and accounts for 40.0% of the variance, while principal component 2 represents the variance between Asc^+ and Asc^- and accounts for 20.2% of the variance. In total, the top five principal components account for nearly 84% of the total variance. Key: cluster 1, control Asc^-; cluster 2, control Asc^+; cluster 3, HI Asc^-; cluster 4, HI Asc^+; cluster 5, HHI Asc^-; cluster 6, HHI Asc^+.

less than one, the standard calculation is applied to generate a negative abundance ratio.

Finally, case C examines the circumstance in which all available cysteines are S-nitrosylated. Before Asc treatment, the fluorescence intensity is zero (background), while after reduction by Asc, the intensity is maximal. The ratio of the two values is very small; therefore, the ratio of ratios is a large negative value. For all cases, any change in protein abundance due to the experimental treatment (control vs test) is normalized by the ratio of ratios, which then reflects the degree of S-nitrosylation of the protein due to the experimental treatment.

Rat Hypoxia-Ischemia/Reperfusion Model. To illustrate this concept experimentally, we have studied endogenous SNO in a rat hypoxia-ischemia (HI)/reperfusion (HHI) model, because S-nitrosylation is widely implicated in ischemic injury, for example, targeting specifically PTEN,[25] as well as apoptosis.[26,27] Neonatal HI is a major cause of neonatal morbidity and mortality and is the most common cause of developmental neurological deficits such as cerebral palsy and delayed cognitive and behavioral deficits such as mental retardation.[28,29] The initial phase following neonatal HI is accompanied by cellular energy failure, membrane depolarization, local release of potentially neurotoxic excitatory neurotransmitters, edema, increase in the intracellular level of calcium, lipid peroxidation, the production of oxygen-free radicals, and decreased blood flow, all of which can lead to cell death.[17,29,30] This initial phase is immediately followed by further neuronal damage, apoptosis, and cerebral edema.

The current clinical treatment for neonatal HI is the use of supraphysiological concentrations of oxygen (HHI) for resuscitation of infants that have been asphyxiated and require assisted ventilation.[31−33] However, recent reports have shown early increases in levels of biochemical markers of oxidative stress after HHI.[34] It has also been shown in animal models that oxygen supplementation after asphyxia increases the rate of formation of free oxygen radicals and decreases cerebral perfusion.[32,35] The Rice−Vannucci model[14] is a clinically relevant model of neonatal HI relying on day P7 rat pups. The lesion is largely restricted to the cerebral hemisphere ipsilateral to the common carotid artery occlusion and is mostly observed in the cerebral parietal cortex and hippocampus.[19] Hyperoxia is an effective resuscitating treatment, but it does not prevent edema, hypoxic insult, brain injury, or motor coordination.[19]

We applied SNOFlo to critically evaluate protein S-nitrosylation in our rat HI/HHI model. We first selected proteins on the basis of the ratios of protein abundance from experimental (Exp) versus control (Ctl) ratios alone. Of the 374 protein spots detected by 2DE, 202 (Exp Asc^-/Ctl Asc^- and Exp Asc^+/Ctl Asc^+, separately) showed statistical significance (ANOVA $p < 0.05$), and all exhibited abundance ratios relative to the controls greater than 1.3. Of these, 164 demonstrated a power of >0.8, and in the

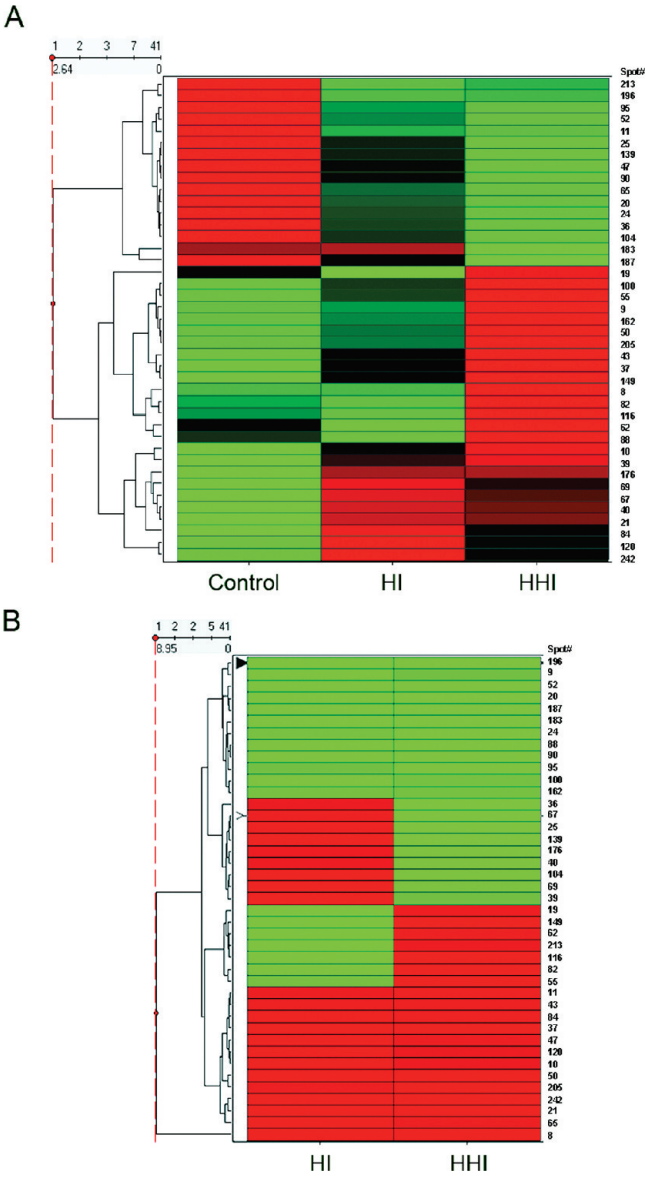

Figure 3. Heat maps of protein spot abundances and ratios of ratios. (A) Protein spot intensities from the Asc^- samples were analyzed as described in the text, and the heat map was generated. Proteins are arrayed vertically with their spot numbers along the right side of the figure. Red indicates spots with positive *Z* scores ($Z > 1.2$), while green indicates spots with negative *Z* scores ($Z < -1.2$) and black intermediate *Z* scores. (B) Ratios of ratios of proteins in panel A. Red indicates spots with positive ratios of ratios (increased R-SH, decreased S-nitrosylation), while green indicates spots with negative ratios of ratios (increased S-nitrosylation, decreased R-SH). Hierarchical clustering was performed with Spotfire. The clustering results are displayed in the form of dendrograms. The row dendrogram (to the left of the diagram) shows the clustering of the proteins, with those clustering together grouped and connected by vertical lines. The horizontal distance is a measure of the dissimilarity in the expression patterns.

effort to minimize false positives, 41 of these satisfied the FDR of <0.05, meaning that two proteins may be falsely discovered in this analysis. Figure 2A shows the average gels of the triplicate samples with the 41 protein spots highlighted with their assigned spot numbers. Principal component analysis (PCA) was performed on the 164 powered (>0.8) protein spots (Figure 2B). PC 1 represents the variance due to controls versus HI and HHI, while PC 2 represents the variance in the data due to the Asc^+ versus Asc^- samples. The figure suggests that most of the variance between HI and HHI samples was due to differences in SNO rather than protein abundance changes, because clusters 3 and 5 (Asc^-) were well separated when compared with clusters 4 and 6 (Asc^+). PC 1 represents ~40% of the variance, while PC 2 represents 20% of the variance in the data set. The top five principal components account for more than 83% of the total variance. This figure emphasizes the need to normalize against protein abundance to extract the SNO response.

To further investigate the relationship of the spots and their abundances, unsupervised cluster analysis was performed and a heat map generated on the basis of the *Z* scores of the FDR subset (41 spots satisfying a FDR, <0.05) of the powered protein spot intensities (Figure 3A). This figure shows the clustering of the proteins with disease severity, the intermediate behavior of the HI rats, and the inverse relationship between the controls and the HHI rats. To complete the analysis, a heat map was generated of the 41 protein spots clustered according to the ratio of ratios (Figure 3B). Clear discrimination between a subset of the proteins between HI and HHI samples is shown. The identities, abundance, statistics, and oxidation state (ratio of ratios and oxidation protective index) of the 41 proteins clustered in panels A and B of Figure 3 are summarized in Table 1. Although the identities of 17 of the 41 proteins selected were questionable (MS expectation scores of >0.001), these were included nevertheless because of their ANOVA and FDR (*q* value) statistics. The FDR values from this collection imply that perhaps no more than two of the 41 proteins were falsely discovered (i.e., null).[24]

Upon HI induction, 26 of the 41 proteins exhibited significant expression ($|\text{abundance}| \geq 1.30$) changes [Table 1, HI expression ratio (Asc^+)]. Upon reperfusion, 25 proteins exhibited significant expression changes [HHI (Asc^+)]. However, 21 proteins showed the greatest changes in SNO (Table 1, ratio of ratios) upon HI induction, while 19 showed the greatest changes in SNO upon HHI. Five identified proteins were found in multiple gel spots (ACTG1, 1MABA, PIAS2, DPYSL3, and TKT), suggesting they were post-translationally modified isoforms, while a sixth remained unidentified (GI: 109506160).

Finally, Ingenuity Pathways Analysis was performed to extract biochemical relationships among the 35 unique proteins and to rationalize their responses to the hypoxic and HHI stressors. Nervous system and cellular development were identified as the top networks that were generated, and the merged network is shown in Figure 4. Of the 35 protein identities submitted, 8 were not functionally identified and 22 were found in the network (Table 1). Functional analysis of the data set included proteins involved in apoptosis (EIF5A, PIAS2, STMN1, NRGN, PDIA3, ALB, NME2, and SCNB); branching morphogenesis of axons (PDIA3), cortical neurons (DPYSL3), and sympathetic neurites (GAP43); neurogenesis (PDIA3, PIAS2, DYPSL3, NRGN, and VIM); and calcium signaling (NRGN, GAP43, and MARCKSL1). Not surprisingly, major abundance changes were also observed for fibrillar proteins known to be stress-responsive in neurons and glia, such as TUBA1C, ACTG1, and VIM.

Comparison of SNOFlo to BST in Defining the Bacterial Nitrosoproteome. The gut lumen represents a complex microenvironment that has the potential to S-nitrosylate bacterial proteins as a means of regulating host−microbe interactions.[2]

Table 1. Rat HI/HHI Model Abundance Summary and Identification[a]

					expression and oxidation ratio[c] (Asc$^-$)		expression ratio (Asc$^+$)		ratio of ratios (Asc−/Asc+)			statistics[f]		
no.	protein name	gene name	accession no.[b]	spot no.	HI[d]	HHI[d]	HI	HHI	HI	HHI	protection index[e]	MS ID score	ANOVA	q value (FDR)
1	eukaryotic translation initiation factor 5A[g,h]	EIF5A	148680528	24	−2.07	−3.47	−1.88	−2.13	−1.10	−1.63	−0.29	3.97×10	3.33×10^{-6}	0.001
2	rCG39881a	EDM18114	149068560	100	1.30	2.06	1.57	2.18	−1.20	−1.06	0.12	5.00×10^{-19}	2.75×10^{-5}	0.001
3	vimentin[h]	VIM	149021114	10	2.11	2.66	1.41	2.58	1.50	1.03	−0.46	2.51×10^{-35}	1.64×10^{-4}	0.001
4	growth-associated protein 43[h]	GAP43	8393415	40	4.26	3.86	4.13	4.58	1.03	−1.19	−0.19	7.92×10^{-28}	2.26×10^{-4}	0.001
5	neurogranin[h]	NRGN	11528516	213	−3.42	−2.89	−2.46	−3.07	−1.39	1.06	0.34	6.29×10^{-14}	3.46×10^{-4}	0.001
6	rCG39881a	EDM18113	149068560	43	1.68	2.81	1.51	2.54	1.11	1.11	0.00	7.92×10^{-13}	1.82×10^{-3}	0.006
7	TRM1 tRNA methyltransferase 1 homologue[g]	TRMT1	149037850	95	−1.43	−1.57	−1.41	−1.14	−1.01	−1.38	−0.26	2.51	4.25×10^{-3}	0.006
8	malate dehydrogenase, mitochondrial[g,h]	MDH2	149063029	8	1.01	3.44	−2.11	−2.45	2.12	8.44	6.32	2.51×10	4.04×10^{-3}	0.013
9	immunity-related GTPase family, Q isoform[h]	IRGQ1	109458349	139	−1.43	−1.79	−1.77	−1.10	1.24	−1.63	−0.63	1.99×10^{-11}	3.07×10^{-3}	0.014
10	tubulin, α 1C[h]	TUBA1C	58865558	176	1.52	1.52	1.46	1.99	1.04	−1.31	−0.27	3.97×10^{-11}	2.45×10^{-3}	0.015
11	rCG57062[g]	EDL90026	149035322	19	−1.52	1.16	1.23	1.09	−1.88	1.06	0.53	6.29×10	2.57×10^{-3}	0.015
12	stathmin 1[h]	STMN1	8393696	90	−1.36	−1.66	−1.12	−1.18	−1.21	−1.40	−0.11	5.00×10^{-38}	3.78×10^{-3}	0.015
13	proteasome subunit, α type[g,h]	PSMA1	149068225	196	−1.35	−1.34	1.45	−1.05	−1.95	−1.27	0.27	1.58	5.10×10^{-2}	0.015
14	chain A, rat liver F1-ATPase	1MABA	6729934	52	−1.80	−2.24	−1.13	−1.03	−1.58	−2.18	−0.17	1.58×10^{-37}	2.14×10^{-2}	0.020
15	transgelin 3[g,h]	TAGLN3	78214333	116	−1.07	1.30	1.30	1.06	−1.39	1.23	0.51	1.58×10	1.70×10^{-3}	0.024
16	rCG39881a	EDM18112	149068560	37	1.89	2.99	1.49	2.45	1.27	1.22	−0.05	1.99×10^{-11}	8.52×10^{-3}	0.024
17	protein inhibitor of activated STAT, 2[g,h]	PIAS2	16758050	25	−2.00	−3.77	−2.31	−2.45	1.16	−1.54	−0.51	7.92×10	5.97×10^{-2}	0.026
18	cordon-bleu (predicted)[g,h]	COBL	149016968	84	1.36	1.22	1.15	1.08	1.18	1.13	−0.05	1.26×10	4.06×10^{-3}	0.028
19	dihydropyrimidinase-like 3b[h]	DPYSL3	149017448	67	2.66	2.37	2.39	3.71	1.11	−1.57	−0.48	1.58×10^{-28}	7.79×10^{-3}	0.028
20	predicted: hypothetical protein[g]	–	109506160	39	1.47	1.61	−1.01	1.63	1.49	−1.01	−0.50	1.99×10	1.02×10^{-2}	0.028
21	actin, γ 1 propeptide	ACTG1	4501887	21	2.89	2.70	1.27	1.90	2.28	1.42	−0.85	1.99×10^{-27}	1.03×10^{-2}	0.028
22	predicted: similar to glyceraldehyde 3-phosphate[g]	–	109480426	187	−1.18	−1.75	1.37	1.10	−1.61	−1.92	−0.10	1.26×10^{-2}	2.25×10^{-2}	0.028
23	predicted: hypothetical protein[g]	–	109506160	36	−2.03	−3.41	−2.06	−1.49	1.01	−2.29	−0.58	6.29	4.41×10^{-2}	0.028
24	dihydropyrimidinase-like 3b[h]	DPYSL3	149017448	104	−1.64	−2.22	−2.07	−1.91	1.26	−1.16	−0.40	1.58×10^{-23}	1.44×10^{-2}	0.029
25	transketolase[h]	TKT	149034223	50	1.16	1.70	−1.09	−1.10	1.26	1.87	0.61	3.15×10^{-8}	9.94×10^{-3}	0.030
26	β-synuclein[h]	SNCB	2501106	20	−2.01	−3.09	−1.23	−1.54	−1.64	−2.01	−0.11	1.99×10^{-22}	2.49×10^{-2}	0.030
27	MARCKS-like 1[g,h]	MARCKSL1	13540687	11	−1.86	−2.04	−2.03	−2.31	1.09	1.13	0.04	7.92×10^{-2}	7.94×10^{-3}	0.031
28	protein disulfide isomerase A3 precursor[h]	PDIA3	1352384	69	1.89	1.66	1.41	1.91	1.33	−1.15	−0.46	1.58×10^{-22}	1.22×10^{-2}	0.033
29	RBL-NDP kinase 18 kDa subunit (p18)[h]	NME2	206580	82	−1.08	1.44	1.20	−1.22	−1.30	1.77	1.00	5.00×10^{-20}	8.73×10^{-3}	0.038
30	actin, γ 1 propeptide	ACTG1	4501887	242	2.02	1.37	−1.07	1.07	2.16	1.29	−0.88	1.99×10^{-11}	1.02×10^{-2}	0.038
31	proteasome subunit, α type[h]	PSMA2	38051991	62	−1.13	1.16	1.30	1.04	−1.47	1.11	0.43	6.29×10^{-15}	1.73×10^{-2}	0.044
32	serum albumin precursor[h]	ALB	124028612	65	−1.57	−1.93	−4.34	−2.12	2.76	1.10	−1.65	5.00×10^{-47}	2.05×10^{-2}	0.044
33	transketolase[h]	TKT	149034223	55	1.07	1.24	1.17	−1.40	−1.10	1.73	0.82	9.98×10^{-7}	1.64×10^{-2}	0.046
34	chain A, rat liver F1-ATPase	1MABA	6729934	162	1.06	1.29	1.17	1.37	−1.10	−1.06	0.04	9.98×10^{-33}	3.40×10^{-2}	0.046
35	protein inhibitor of activated STAT, 2[g,h]	PIAS2	16758050	47	−1.68	−2.68	−2.38	−2.92	1.42	1.09	−0.33	7.92×10	1.00×10^{-1}	0.046

dx.doi.org/10.1021/bi200008b |*Biochemistry* 2011, 50, 5601–5614

Table 1. Continued

no.	protein name	gene name	accession no.[b]	spot no.	expression and oxidation ratio[c] (Asc$^-$)		expression ratio (Asc$^+$)		ratio of ratios (Asc−/Asc+)			statistics[f]		
					HI[d]	HHI[d]	HI	HHI	HI	HHI	protection index[e]	MS ID score	ANOVA	q value (FDR)
36	predicted: hypothetical protein isoform 1[g]	–	109512929	205	1.15	1.68	1.05	−1.24	1.10	2.08	0.98	9.98×10	2.33×10^{-2}	0.049
37	RAB16a[h]	RAB3D	206539	149	1.26	1.60	1.99	1.29	−1.58	1.23	0.60	1.99	9.49×10^{-3}	0.050
38	rCG50513a[g]	EDL87015	149032103	88	−1.06	1.13	1.14	1.64	−1.21	−1.45	−0.14	7.92×10^{-1}	1.38×10^{-2}	0.050
39	fatty acid-binding protein	FABPII	404382	9	1.21	2.21	2.41	2.23	−1.99	−1.01	0.49	7.92×10^{-12}	2.90×10^{-2}	0.050
40	rCG25966a[g]	EDL77699	149019058	120	1.60	1.20	1.06	1.19	1.51	1.01	−0.50	1.58×10	3.45×10^{-2}	0.050
41	endoplasmic reticulum protein 29a[h]	ERP29	149063414	183	1.00	−1.08	1.40	1.55	−1.40	−1.67	−0.12	5.00×10^{-9}	3.71×10^{-2}	0.050

[a] The table summarizes the expression ratios, protection index, expression statistics, and MS identification data and statistics. The protection index is defined as the difference in the ratios of ratios (defined in the legend of Figure 1) between the two treatments. [b] GI number. [c] For the sake of clarity, expression ratio is defined here as the abundance ratio of total protein (Asc+) in either the HI or HHI relative to the control protein abundance. [d] HI, hypoxia-ischemia; HHI, hypoxia-ischemia/reperfusion. Negative values reflect the negative inverse of abundance ratios of <1.0. [e] Protection index is the difference between the HHI and HI ratios before conversion to the negative inverse as described for footnote c. [f] Statistics for Asc$^-$ abundance data. [g] MS ID expectation score cutoff of >0.001. [h] Proteins in Nervous System Development and Function network (see Figure 4).

Potential sources of S-nitrosylating agents include dietary nitrates and heme, cellular and microbially derived nitric oxide, and S-nitrosylated proteins and peptides. We have previously reported that stimulated glial cells in the gut regulate intestinal inflammation via the secretion of GSNO, which is a potent transnitrosylating agent.[36] The S-nitrosylating potential of the gut lumen is elevated further by the activation of nitric oxide synthases during inflammation and infection and confers a potentially important disease-modulating role. However, at present, it remains unclear whether such immunomodulatory SNO signals, or indeed how pharmacological doses of antimicrobial GSNO,[2] may also act on bacterial virulence factors in the gut lumen.

To address this possibility and to validate SNOFlo as a method for the quantitative detection of SNO, we extracted native proteins from enteropathogenic *E. coli* (EPEC) using chloroform-osmotic shock and treated this preparation under nonreducing conditions with GSNO (1−100 μM, ranging from physiologic to pharmacologic concentrations) to identify microbial proteins that are readily S-nitrosylated molecular targets. Pilot studies demonstrated similarly elevated bacterial protein S-nitrosylation profiles over this GSNO concentration range [<5 μM being physiologic in the GI tract (unpublished findings)], and a robust 100 μM antimicrobial pharmacologic dose was chosen to demonstrate proof of concept. Protein SNO specificity was additionally demonstrated by SNO photolysis of the GSNO labeling (UV; 302 nm for 10 min at 9000 μW/cm^2), which yielded a similar reduction to ascorbate [1−20 mM (Figure S1 of the Supporting Information)]. GSNO-treated versus untreated extracts were analyzed by 2DE, and 25 spots with higher labeling intensity in the GSNO treatment group were selected and identified by mass spectrometry. The SNO proteins identified by our method (Table 2) included those involved in protein synthesis (E-Tu and RF4), folding (rotamase B and DnaK), global regulation (NHS and SodB), quorum sensing (LuxS), signal transduction (four kinases), and bacterial attachment (OmpA and OmpX). Twenty of the 25 identified proteins harbored the minimal sequence motif for SNO (cysteine adjacent to an Asp or Glu).[37] Many of the SNO proteins identified were of cytoplasmic origin, which is not surprising because this represents a rich source of cysteine-containing proteins, and chloroform treatment of *E. coli* cells releases cytoplasmic and cytoplasmic membrane (CM)-associated proteins below 100 kDa via mechanosensitive MscL channels[37] [including elongation factor Tu (E-Tu) and molecular chaperone DnaK]. Fourteen of the identified proteins (Table 2) have been previously indicated as targets for SNO in other organisms, indirectly validating our method.

Further, to critically compare SNOFlo with the popular BST, we analyzed bacterial SNO labeling using the two different methods by 2DE. Direct comparison of the BST and BD-labeled protein populations produced very different patterns because for every cysteine labeled, the biotin moiety imparts a pK_a of 4.66, thereby altering the pI of the proteins modified. By contrast, the SNOFlo method does not alter the pI of modified proteins.

DISCUSSION

We have presented an alternative quantitative, reproducible, and sensitive method for establishing the S-nitrosylated state of cysteines, in both in vitro and in vivo models. Our approach described here builds on our previously published methods that

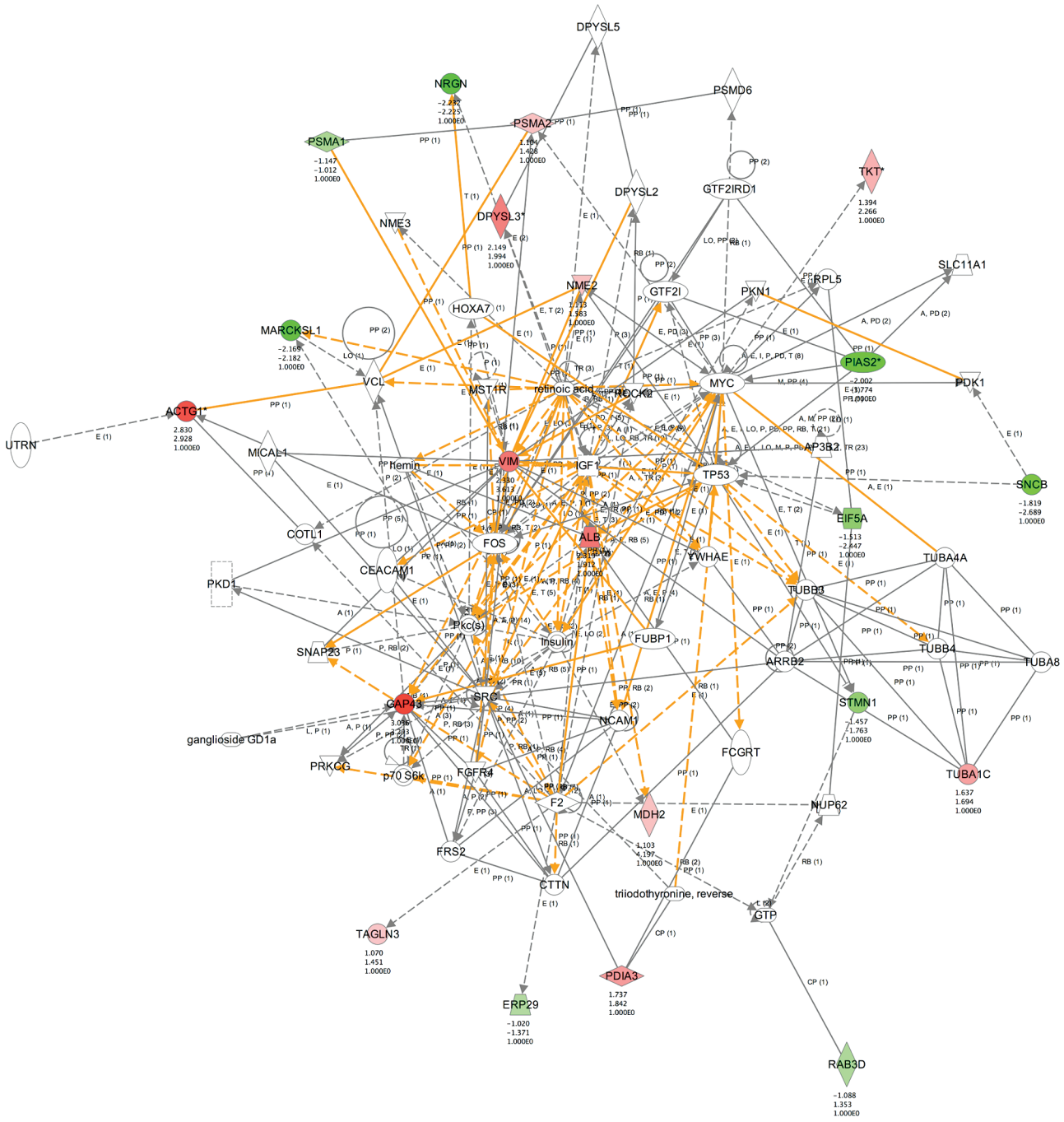

Figure 4. Ingenuity pathway analysis of identified proteins in the rat HHI model. Protein ID's were submitted to Ingenuity Pathway Systems (Ingenuity Systems, http://www.ingenuity.com), along with their protection indices. The top pathway generated by IPA is represented here and was identified as the nervous system development and function pathway. Of the 35 unique proteins exhibiting significance (Table 1), 23 play a role in this pathway and are colored (red for positive PI and green for negative PI), and their PIs are listed below their location in the pathway.

are specifically targeted to investigations of global proteomic inquiry.[11,12] Recognizing that more than 90% of human proteins contain at least one cysteine,[38] the strategy is based upon cysteine-specific, truly saturation labeling with uncharged fluorescent dyes for addressing quantification in unbiased differential proteomics investigations. Important considerations for unbiased differential proteomics investigations include the impact of the modification on electrophoretic mobility or chromatographic selectivity and the need for high sensitivity.

To minimize sample manipulation, such as precipitations and adsorptive chromatography before samples are labeled, our approach permits electrophoresis immediately after labeling without removal of unincorporated (but passivated) dye. Free dye diffuses out of the medium during IEF incubation, and the remainder migrates off the 2D gel during electrophoresis. However, dialysis is required to remove ascorbate prior to the labeling step (as ascorbate interferes with maleimide labeling), but this methodology represents a significant advance over existing

Table 2. GSNO-Treated Bacterial Proteins Identified by SNOFlo[a]

no.	protein name	gene name	accession no.[b]	spot no.	no. of cysteines[c]	cysteine-containing peptides[d]
1	DnaK transcriptional regulator	dksA	215485305	4	4	FGYCESCGVE, ADLCIDCKTL
2	*S*-ribosylhomocysteinase	luxS	215488011	5	3	LRFCVPN, PMGCRTG, VYQCGTY
3	elongation factor P	efp	215489494	6	1	QAECIVT
4	superoxide dismutase	sodB	215486832	7	1	YWNCLAP
5	outer membrane protein X	ompX	215485901	10	1	KIACLSA
6	peptidyl-prolyl *cis*−*trans* isomerase B	ppiB	215485602	11	2	LDYCREG, WGYCVFA
7	nucleoside diphoshate kinase	ndk	215487868	12	1	GEVCPRT
8	ribosome recycling factor	frr	215485333	13	1	MDKCVEA
9	adenylate kinase	adk	215485554	14	1	QEDCRNG
10	uridine phosphorylase	udp	215489172	15	3	VIVCSTG, DFECTTA, LTMCASG
11	outer membrane protein A	ompA	215486075	16	2	GNTCDNV, LIDCLAP
12	molecular chaperone	dnaK	215485175	17	1	TNSCVAI
13	elongation factor Tu	tufA	215488625	18	3	HVDCPGH, LNKCDMV, KSTCTGV
14	elongation factor G	fusA	215488626	20	3	MVYCAVG, LVTCGSA, DTLCDPD
15	phosphoenolpyruvate carboxykinase	pckA	215488683	21	4	DAFCGAN, GAKCTNP, EGGCYAK, FSACFGA
16	elongation factor Tu	tufA	215488625	22	3	HVDCPGH, LNKCDMV, KSTCTGV
17	phosphoglycerate kinase	pgk	215488219	23	3	AALCDVF, DVACAGP, LTTCNIP
18	elongation factor Ts	tsf	215485331	24	2	MMDCKKA, EVNCQTD
19	alkyl hydroperoxide reductase subunit C	ahpC	215485649	25	2	TFVCPTE, GEVCPAK
20	elongation factor Tu	tufB	215489312	26	3	HVDCPGH, LNKCDMV, KSTCTGV

[a] The table shows the 20 most intensely stained *E. coli* E2348/69 proteins from 2DE gels, which were picked and identified by MS. The table also shows the number of cysteines calculated from corresponding protein sequences as well as the sequences around the cysteines harboring the putative minimal sequential S-nitrosylation motif (Cys with adjacent Asp or Glu). [b] GI number. [c] Number of cysteines in the protein sequence. [d] Protein sequence around the cysteines.

technology. Furthermore, recognizing that the reproducibility and accuracy of quantification require modifications that ensure true saturation, our approach estimates the cysteine content of the entire protein extract by amino acid analysis and incubates the extract with a 60-fold molar excess of dye over protein thiol. Strict pH control (pH 7.5) is maintained to minimize non-cysteine modifications, even for dye:protein thiol ratios of 100:1. Finally, any modification that alters the electrophoretic mobility of proteins, or LC retention time for peptides, greatly diminishes the ability to match across the experiment, particularly when variable degrees of modification are present. This is critical for SNO quantification, where the amount of protein-bound fluorescent label reflects the degree of initial SNO modification and may vary due to the experimental goals. In our approach, the uncharged character of BD permits direct estimation of protein intensity between samples regardless of whether the proteins' cysteines are unmodified, partially modified, or fully modified while at the same time allowing the calculation of the ratio of ratios to normalize for changes in protein abundance and changes in SNO due to the experimental design.

Specifically with respect to the BST strategy, some concerns have been raised that the use of Asc may reverse not only nitrosylation but also other modifications of protein thiols. For example, it has been shown that Asc reduces the sulfenic acid form of the catalytic cysteine of yeast peroxiredoxin 1,[39] returning it to an active state. As a result, our studies presented here may have quantified total Asc-reversible cysteine modifications (excepting disulfide reduction), rather than specifically S-nitrosylation. Others have observed false positive signals in samples for which no S-nitrosylation has occurred,[40,41] or which suggest reduction of glutathione-adducted cysteines.[42] These observations initiated a directed study that concluded that false positive signals might have originated from denitrosylation of endogenous SNOs by indirect sunlight,[43] which is known to cause loss of the unstable SNO. This study demonstrated the profound ascorbate dependency of the BST and specificity of ascorbate (up to 100 mM) for protein SNO. However, this phenomenon does not explain the observed reactivity of completely reduced and S-alkylated proteins.[40] It is possible that this discrepancy may be due to incomplete protein denaturation in the latter study, because SNO may be quite stable in structurally intact proteins.[44] Moreover, several reports have recently demonstrated transition metal ion dependency of the BST, with ascorbate−metal ion complexes showing specificity for protein SNO, and not for other oxidative cysteinyl modifications, including disulfides.[45−49] It may therefore be possible to significantly enhance the sensitivity of SNOFlo by simple sample assay addition of metal ions to the ascorbate reduction step.[49] In support of this notion, we demonstrate enhanced reversal of GSNO-induced protein SNO by ascorbate copper I ions versus ascorbate alone and confirm the specificity by SNO photolysis[41] (Figure S1 of the Supporting Information). Until the ascorbate specificity for protein SNO is unanimously authenticated for BST or alternative reducing agents are implemented,[50] protein targets should ideally be validated using techniques such as selected reaction monitoring, as these provide unequivocal demonstration of the cysteinyl modification.

In addition to the value of the calculation of the ratio of ratios in indicating the Asc-reversible modifications of cysteines, an important corollary is the change in the ratio of ratios as a result of the treatment, a concept we note as the oxidation protection index (PI; a positive value as a result of a treatment is correlated with an increased level of free sulfhydryls, hence "protection" against oxidation). While the ratio of ratios for a given protein

under a given biological treatment indicates the degree of modification, when a different biological treatment (or time course) results in a change in this degree of modification, then important information relating to the protein and its role in the biology of the oxidative challenge may be implied. Thus, a series of targeted experiments to further characterize and illuminate its role or mechanism of action may be indicated by calculation of the PI.

Of great interest was the involvement of three calmodulin (CaM)-binding proteins (NRGN, GAP43, and MARCKSL1) found to respond to HI and HHI in this study. The first two are members of the calpacitin protein family whose apparent function is to bind calmodulin in the presence of low levels of calcium, regulating its availability. Both are substrates for PKCγ, which upon phosphorylation release CaM. This activity has been proposed to directly govern plasticity in mice by determining the kinetics and magnitude of the response to calcium.[51] Of relevance to this study is the fact that in response to S-glutathionylation, the binding affinity of NRGN for PKC is lower than that of its unmodified form, while that of GAP43 is higher than that of its unmodified form.[52] Our study shows that the PI values for these two proteins are also inversely correlated; i.e., in response to HHI, GAP43 exhibits a negative PI (−0.19, shift toward SNO), while NRGN exhibits a positive PI (0.34, shift toward the reduced SH). These observations suggest that, although opposite in nature, both shifts result in NRGN and GAP43 states that are more favorable for PKC phosphorylation and release of CaM, which may play a role in the augmentation of inflammation and edema by hypoxia.[18,19]

What is more intriguing is the involvement of ER protein 29, a chaperone protein most likely playing a role in the stress response mechanisms associated with HI and HHI, as well as the involvement of MDH2, and STMN1, given that there is evidence of a shift from mitochondrial apoptotic signaling to ER death signaling with more necrotic features after HI.[18] Proteosome activity (PSMA1 and PSMA2) was also involved, not surprisingly given the cell death responses exhibited by HI[16] and HHI.[18]

Also of interest is the response of protein disulfide isomerase (PDIA3) to HI and HHI. This protein is found on the cell surface and has been shown to catalyze the transfer of extracellular NO to intracellular protein thiols near the membrane.[53,54] It also catalyzes sulfhydryl oxidization of newly synthesized proteins to aid in proper folding and is kept in the oxidized state in the endoplasmic reticulum. In the absence of oxygen (HI), proteins may be misfolded, triggering the unfolded protein response process that ultimately leads to proteosomal degradation.[55] In our study, PDIA3 shifts from a reduced state under HI to an oxidized state under HHI (PI = −1.15).

At the risk of overinterpretation, these results might imply that cysteine S-nitrosylation plays a significant role in the coordination of phosphorylation pathways known to regulate calcium fluxes and subsequent cell death phenotypes and inflammation, as well as neuronal cell development in general. This will require, however, more detailed investigation and at this stage is speculative. These studies have been made possible by the use of saturating conditions for fluorescence labeling and the use of an uncharged dye to permit direct and quantitative comparisons and matching of protein spots in unbiased proteomics investigations. It is our belief that the SNOFlo procedure can be put to good use in further illuminating the role of SNO in the regulation of cellular signaling systems.

■ ASSOCIATED CONTENT

Supporting Information. BST as described in Experimental Procedures with *E. coli* E2348/69 cell extract (Figure S1). Two micrograms of protein per lane was loaded onto a 4 to 20% gradient SDS gel. Detection with IRDye800 streptavidin and Licor Odyssey at 800 nm: lane 1, nontreated control; lane 2, sample treated with 100 μM GSNO; lanes 3−5, samples after 100 μM GSNO treatment with 1 mM ascorbate and 1 μM CuI, SNO photolysis, and 20 mM ascorbate, respectively, before blocking. This material is available free of charge via the Internet at http://pubs.acs.org.

■ AUTHOR INFORMATION

Corresponding Author

*Phone: (409) 772-2764. Fax: (409) 772-8025. E-mail: jowiktor@utmb.edu.

Funding Sources

This work was supported in part by National Heart, Lung, and Blood Institute Proteomics Center Contract N01-HV-00245 (A.K.), National Institute of Diabetes and Digestive and Kidney Diseases Grants R21-DK078032-01 (T.C.S.) and 1UL1RR029876-01 (T.C.S.), the Eli and Edythe Broad Foundation (T.C.S.), and National Institute of Child Health and Human Development Grant PO1-HDO039833 (J.R.P.-P.).

■ ACKNOWLEDGMENT

We acknowledge the excellent technical assistance provided by Drs. Zheng Wu, Robert English, and Anthony Haag and Mr. J. Steve Smith of the University of Texas Medical Branch Biomolecular Resource Facility.

■ ABBREVIATIONS

SNO, cysteinyl S-nitrosylation; NO, nitric oxide; BST, biotin-switch technique; MMTS, methylmethane thiosulfonate; Asc, ascorbate; 2DE, two-dimensional gel electrophoresis; SNOFlo, SNO detection by fluorescence; BD, BODIPY FL *N*-(2-aminoethyl)maleimide; HI, hypoxia-ischemia; HHI, hypoxia-ischemia/reperfusion; GSNO, S-nitrosylated glutathione; FDR, false discovery rate; PCA, principal component analysis; EPEC, enteropathogenic *E. coli*; CM, cytoplasmic-membrane; PI, oxidation protection index; CaM, calmodulin; DTPA, diethylenetriaminepentaacetic acid; UPGMA, unweighted pair group method with the arithmetic mean.

■ REFERENCES

(1) Torta, F., Usuelli, V., Malgaroli, A., and Bachi, A. (2008) Proteomic analysis of protein S-nitrosylation. *Proteomics 8*, 4484–4494.

(2) Foster, M. W., Hess, D. T., and Stamler, J. S. (2009) Protein S-nitrosylation in health and disease: A current perspective. *Trends Mol. Med. 15*, 391–404.

(3) Lopez-Sanchez, L. M., Muntane, J., de la Mata, M., and Rodriguez-Ariza, A. (2009) Unraveling the S-nitrosoproteome: Tools and strategies. *Proteomics 9*, 808–818.

(4) Lima, B., Forrester, M. T., Hess, D. T., and Stamler, J. S. (2010) S-nitrosylation in cardiovascular signaling. *Circ. Res. 106*, 633–646.

(5) Mannick, J. B., Hausladen, A., Liu, L., Hess, D. T., Zeng, M., Miao, Q. X., Kane, L. S., Gow, A. J., and Stamler, J. S. (1999) Fas-induced caspase denitrosylation. *Science 284*, 651–654.

(6) Gow, A., Doctor, A., Mannick, J., and Gaston, B. (2007) S-Nitrosothiol measurements in biological systems. *J. Chromatogr., B: Anal. Technol. Biomed. Life Sci. 851*, 140–151.

(7) Jaffrey, S. R., Erdjument-Bromage, H., Ferris, C. D., Tempst, P., and Snyder, S. H. (2001) Protein S-nitrosylation: A physiological signal for neuronal nitric oxide. *Nat. Cell Biol. 3*, 193–197.

(8) Jaffrey, S. R., Fang, M., and Snyder, S. H. (2002) Nitrosopeptide mapping: A novel methodology reveals S-nitrosylation of dexras1 on a single cysteine residue. *Chem. Biol. 9*, 1329–1335.

(9) Sun, J., Morgan, M., Shen, R. F., Steenbergen, C., and Murphy, E. (2007) Preconditioning results in S-nitrosylation of proteins involved in regulation of mitochondrial energetics and calcium transport. *Circ. Res. 101*, 1155–1163.

(10) Kettenhofen, N. J., Broniowska, K. A., Keszler, A., Zhang, Y., and Hogg, N. (2007) Proteomic methods for analysis of S-nitrosation. *J. Chromatogr., B: Anal. Technol. Biomed. Life Sci. 851*, 152–159.

(11) Pretzer, E., and Wiktorowicz, J. E. (2008) Saturation fluorescence labeling of proteins for proteomic analyses. *Anal. Biochem. 374*, 250–262.

(12) Tyagarajan, K., Pretzer, E. L., and Wiktorowicz, J. E. (2003) Thiol-reactive dyes for fluorescence labeling of proteomic samples. *Electrophoresis 24*, 2348–2358.

(13) Jamaluddin, M., Wiktorowicz, J. E., Soman, K. V., Boldogh, I., Forbus, J. D., Spratt, H., Garofalo, R. P., and Brasier, A. R. (2010) Role of Peroxiredoxin-1 and -4 in Protection of RSV-induced Cysteinyl-oxidation of Nuclear Cytoskeletal Proteins. *J. Virol. 84*, 9533–9545.

(14) Rice, J. E., III, Vannucci, R. C., and Brierley, J. B. (1981) The influence of immaturity on hypoxic-ischemic brain damage in the rat. *Ann. Neurol. 9*, 131–141.

(15) Grafe, M. R. (1994) Developmental changes in the sensitivity of the neonatal rat brain to hypoxic/ischemic injury. *Brain Res. 653*, 161–166.

(16) Hu, X., Qiu, J., Grafe, M. R., Rea, H. C., Rassin, D. K., and Perez-Polo, J. R. (2003) Bcl-2 family members make different contributions to cell death in hypoxia and/or hyperoxia in rat cerebral cortex. *Int. J. Dev. Neurosci. 21*, 371–377.

(17) Hu, X., Rea, H. C., Wiktorowicz, J. E., and Perez-Polo, J. R. (2006) Proteomic analysis of hypoxia/ischemia-induced alteration of cortical development and dopamine neurotransmission in neonatal rat. *J. Proteome Res. 5*, 2396–2404.

(18) Gill, M. B., Bockhorst, K., Narayana, P., and Perez-Polo, J. R. (2008) Bax shuttling after neonatal hypoxia-ischemia: Hyperoxia effects. *J. Neurosci. Res. 86*, 3584–3604.

(19) Ferrari, D. C., Nesic, O. B., and Perez-Polo, J. R. (2010) Oxygen resuscitation does not ameliorate neonatal hypoxia/ischemia-induced cerebral edema. *J. Neurosci. Res. 88*, 2056–2065.

(20) Iguchi, A., Thomson, N. R., Ogura, Y., Saunders, D., Ooka, T., Henderson, I. R., Harris, D., Asadulghani, M., Kurokawa, K., Dean, P., Kenny, B., Quail, M. A., Thurston, S., Dougan, G., Hayashi, T., Parkhill, J., and Frankel, G. (2009) Complete genome sequence and comparative genome analysis of enteropathogenic *Escherichia coli* O127:H6 strain E2348/69. *J. Bacteriol. 191*, 347–354.

(21) Ames, G. F.-L., Brody, C., and Kustu, S. (1984) Simple, rapid, and quantitative release of periplasmic proteins by chloroform. *J. Bacteriol. 160*, 1181–1183.

(22) Jaffrey, S. R., and Snyder, S. H. (2001) The Biotin Switch Method for the detection of S-nitrosylated proteins. *Sci. STKE 86*, 1–10.

(23) Turck, C. W., Falick, A. M., Kowalek, J. A., Lane, W. S., Lilley, K. S., Phinney, B. S., Weintraub, S. T., Witkowska, H. E., and Yates, N. A. (2006) ABRF-PRG06: Relative Protein Quantification. In *Association of Biomolecular Resource Facilities 2006*, Long Beach, CA.

(24) Storey, J. D., and Tibshirani, R. (2003) Statistical significance for genomewide studies. *Proc. Natl. Acad. Sci. U.S.A. 100*, 9440–9445.

(25) Pei, D. S., Sun, Y. F., and Song, Y. J. (2009) S-Nitrosylation of PTEN involved in ischemic brain injury in rat hippocampal CA1 region. *Neurochem. Res. 34*, 1507–1512.

(26) Duan, S., Wan, L., Fu, W. J., Pan, H., Ding, Q., Chen, C., Han, P., Zhu, X., Du, L., Liu, H., Chen, Y., Liu, X., Yan, X., Deng, M., and Qian, M. (2009) Nonlinear cooperation of p53-ING1-induced bax expression and protein S-nitrosylation in GSNO-induced thymocyte apoptosis: A quantitative approach with cross-platform validation. *Apoptosis 14*, 236–245.

(27) Kolb, J. P. (2001) Pro- and anti-apoptotic role of nitric oxide, NO. *C. R. Acad. Sci., Ser. III 324*, 413–424.

(28) Boichot, C., Walker, P. M., Durand, C., Grimaldi, M., Chapuis, S., Gouyon, J. B., and Brunotte, F. (2006) Term neonate prognoses after perinatal asphyxia: Contributions of MR imaging, MR spectroscopy, relaxation times, and apparent diffusion coefficients. *Radiology 239*, 839–848.

(29) Zanelli, S. A., Stanley, D. P., and Kaufman, D. A. (2008) Hypoxic-Ischemic Encephalopathy. http://emedicine.medscape.com/article/973501-overview.

(30) Calvert, J. W., and Zhang, J. H. (2005) Pathophysiology of an hypoxic-ischemic insult during the perinatal period. *Neurol. Res. 27*, 246–260.

(31) Deulofeut, R., Critz, A., Adams-Chapman, I., and Sola, A. (2006) Avoiding hyperoxia in infants < or = 1250 g is associated with improved short- and long-term outcomes. *J. Perinatol. 26*, 700–705.

(32) Koch, J. D., Miles, D. K., Gilley, J. A., Yang, C. P., and Kernie, S. G. (2008) Brief exposure to hyperoxia depletes the glial progenitor pool and impairs functional recovery after hypoxic-ischemic brain injury. *J. Cereb. Blood Flow Metab. 28*, 1294–1306.

(33) Wang, C. L., Anderson, C., Leone, T. A., Rich, W., Govindaswami, B., and Finer, N. N. (2008) Resuscitation of preterm neonates by using room air or 100% oxygen. *Pediatrics 121*, 1083–1089.

(34) Klinger, G., Beyene, J., Shah, P., and Perlman, M. (2005) Do hyperoxaemia and hypocapnia add to the risk of brain injury after intrapartum asphyxia? *Arch. Dis. Child. 90* (Fetal Neonatal Edition), F49–F52.

(35) Ahn, E. S., Robertson, C. L., Vereczki, V., Hoffman, G. E., and Fiskum, G. (2008) Normoxic ventilatory resuscitation following controlled cortical impact reduces peroxynitrite-mediated protein nitration in the hippocampus. *J. Neurosurg. 108*, 124–131.

(36) Savidge, T. C., Newman, P., Pothoulakis, C., Ruhl, A., Neunlist, M., Bourreille, A., Hurst, R., and Sofroniew, M. V. (2007) Enteric glia regulate intestinal barrier function and inflammation via release of S-nitrosoglutathione. *Gastroenterology 132*, 1344–1358.

(37) Stamler, J. S., Toone, E. J., Lipton, S. A., and Sucher, N. J. (1997) (S)NO signals: Translocation, regulation, and a consensus motif. *Neuron 18*, 691–696.

(38) Miseta, A., and Csutora, P. (2000) Relationship between the Occurrence of Cysteine in Proteins and the Complexity of Organisms. *Mol. Biol. Evol. 17*, 1232–1239.

(39) Monteiro, G., Horta, B. B., Pimenta, D. C., Augusto, O., and Netto, L. E. (2007) Reduction of 1-Cys peroxiredoxins by ascorbate changes the thiol-specific antioxidant paradigm, revealing another function of vitamin C. *Proc. Natl. Acad. Sci. U.S.A. 104*, 4886–4891.

(40) Huang, B., and Chen, C. (2006) An ascorbate-dependent artifact that interferes with the interpretation of the biotin switch assay. *Free Radical Biol. Med. 41*, 562–567.

(41) Giustarini, D., Dalle-Donne, I., Colombo, R., Milzani, A., and Rossi, R. (2008) Is ascorbate able to reduce disulfide bridges? A cautionary note. *Nitric Oxide 19*, 252–258.

(42) Dahm, C. C., Moore, K., and Murphy, M. P. (2006) Persistent S-nitrosation of complex I and other mitochondrial membrane proteins by S-nitrosothiols but not nitric oxide or peroxynitrite: Implications for the interaction of nitric oxide with mitochondria. *J. Biol. Chem. 281*, 10056–10065.

(43) Forrester, M. T., Foster, M. W., and Stamler, J. S. (2007) Assessment and application of the biotin switch technique for examining protein S-nitrosylation under conditions of pharmacologically induced oxidative stress. *J. Biol. Chem. 282*, 13977–13983.

(44) Paige, J. S., Xu, G., Stancevic, B., and Jaffrey, S. R. (2008) Nitrosothiol reactivity profiling identifies S-nitrosylated proteins with unexpected stability. *Chem. Biol. 15*, 1307–1316.

(45) Chouchani, E. T., Hurd, T. R., Nadtochiy, S. M., Brookes, P. S., Fearnley, I. M., Lilley, K. S., Smith, R. A., and Murphy, M. P. (2010) Identification of S-nitrosated mitochondrial proteins by S-nitrosothiol difference in gel electrophoresis (SNO-DIGE): Implications for the regulation of mitochondrial function by reversible S-nitrosation. *Biochem. J. 430*, 49–59.

(46) Nadtochiy, S. M., Burwell, L. S., Ingraham, C. A., Spencer, C. M., Friedman, A. E., Pinkert, C. A., and Brookes, P. S. (2009) In vivo cardioprotection by S-nitroso-2-mercaptopropionyl glycine. *J. Mol. Cell. Cardiol. 46*, 960–968.

(47) Sanghani, P. C., Davis, W. I., Fears, S. L., Green, S. L., Zhai, L., Tang, Y., Martin, E., Bryan, N. S., and Sanghani, S. P. (2009) Kinetic and cellular characterization of novel inhibitors of S-nitrosoglutathione reductase. *J. Biol. Chem. 284*, 24354–24362.

(48) Straub, A. C., Billaud, M., Johnstone, S. R., Best, A. K., Yemen, S., Dwyer, S. T., Looft-Wilson, R., Lysiak, J. J., Gaston, B., Palmer, L., and Isakson, B. E. (2011) Compartmentalized connexin 43 S-nitrosylation/denitrosylation regulates heterocellular communication in the vessel wall. *Arterioscler., Thromb., Vasc. Biol. 31*, 399–407.

(49) Wang, X., Kettenhofen, N. J., Shiva, S., Hogg, N., and Gladwin, M. T. (2008) Copper dependence of the biotin switch assay: Modified assay for measuring cellular and blood nitrosated proteins. *Free Radical Biol. Med. 44*, 1362–1372.

(50) Kallakunta, V. M., Staruch, A., and Mutus, B. (2010) Sinapinic acid can replace ascorbate in the biotin switch assay. *Biochim. Biophys. Acta 1800*, 23–30.

(51) Krucker, T., Siggins, G. R., McNamara, R. K., Lindsley, K. A., Dao, A., Allison, D. W., De Lecea, L., Lovenberg, T. W., Sutcliffe, J. G., and Gerendasy, D. D. (2002) Targeted disruption of RC3 reveals a calmodulin-based mechanism for regulating metaplasticity in the hippocampus. *J. Neurosci. 22*, 5525–5535.

(52) Li, J., Huang, F. L., and Huang, K. P. (2001) Glutathiolation of proteins by glutathione disulfide S-oxide derived from S-nitrosoglutathione. Modifications of rat brain neurogranin/RC3 and neuromodulin/GAP-43. *J. Biol. Chem. 276*, 3098–3105.

(53) Sliskovic, I., Raturi, A., and Mutus, B. (2005) Characterization of the S-denitrosation activity of protein disulfide isomerase. *J. Biol. Chem. 280*, 8733–8741.

(54) Ramachandran, N., Root, P., Jiang, X. M., Hogg, P. J., and Mutus, B. (2001) Mechanism of transfer of NO from extracellular S-nitrosothiols into the cytosol by cell-surface protein disulfide isomerase. *Proc. Natl. Acad. Sci. U.S.A. 98*, 9539–9544.

(55) Tu, B. P., and Weissman, J. S. (2004) Oxidative protein folding in eukaryotes: Mechanisms and consequences. *J. Cell Biol. 164*, 341–346.